

We are IntechOpen, the world's leading publisher of Open Access books Built by scientists, for scientists

6,900

Open access books available

186,000

International authors and editors

200M

Downloads

Our authors are among the

154

Countries delivered to

TOP 1%

most cited scientists

12.2%

Contributors from top 500 universities



WEB OF SCIENCE™

Selection of our books indexed in the Book Citation Index
in Web of Science™ Core Collection (BKCI)

Interested in publishing with us?
Contact book.department@intechopen.com

Numbers displayed above are based on latest data collected.
For more information visit www.intechopen.com



Magnetic and Electric Properties of Organic Nitroxide Radical Liquid Crystals and Ionic Liquids

Rui Tamura, Yoshiaki Uchida and Katsuaki Suzuki

Additional information is available at the end of the chapter

<http://dx.doi.org/10.5772/39120>

1. Introduction

Amongst stable organic free radicals such as nitroxides, verdazyls, thioaminyls, a certain hydrazyl, phenoxyls, and carbon-centered radicals, nitroxide radicals (NRs) show outstanding thermodynamic stability ascribed to the delocalization of the unpaired electron over the N–O bond and thereby no dimerization (Aurich, 1989; Hicks, 2010). In fact, sterically protected NRs have found various practical applications in the field of materials science. The landmark is the discovery by Kinoshita et al. in 1991 of the first purely organic ferromagnet ($T_c = 0.6$ K) with respect to one of several polymorphs of a nitronyl nitroxide, 2-(4-nitrophenyl)-4,4,5,5-tetramethylimidazoline-1-oxy-3-oxide (**1**) (Figure 1) (Tamura et al., 1991). Since then, stable NR structures have been used as the spin source and building block for the elaboration of organic or molecule-based magnetic materials. Up to the late 1990s, more than 20 NR-based organic ferromagnets were prepared (Amabilino & Veciana, 2001); the highest T_c value of 1.48 K was recorded for one of polymorphs of 1,3,5,7-tetramethyl-2,6-diazaadamane-*N,N'*-dioxy (**2**) prepared by Rassat et al. in 1993 (Figure 1) (Chiarelli et al., 1993). Furthermore, to verify the theoretical prediction for constructing organoferromagnetic conductor, several donors and acceptors carrying NR units were prepared to give the corresponding CT complexes and radical salts (Nakatsuji, 2008). In 2007, Matsushita et al. reported that a radical ion salt of a tetrathiafulvalene (TTF)-based spin-polarized donor NR compound (**3**) successfully exhibited giant negative magnetoresistance, i.e., the decrease in the resistance of the salt by more than 70% under a magnetic field of 9 T at 2K (Figure 1) (Matsushita et al., 2007, 2008). This is the first example detecting the interaction between localized spins and conducting electrons in an organic molecular assembly, i.e., a molecule-based spintronics using not only the charge but also the spin of an electron (Sugawara et al., 2011). Meanwhile, for the last decade the redox

properties of NRs have been utilized for the development of environmentally benign organic cathode-active materials for rechargeable batteries with a high energy-density, such as a stable nitroxide polyradical, poly(2,2,6,6-tetramethylpiperidinyloxy methacrylate) (**4**) (Figure 1) (Nakahara, 2002; Oyaizu & Nishide, 2010; Suga & Nishide, 2010).

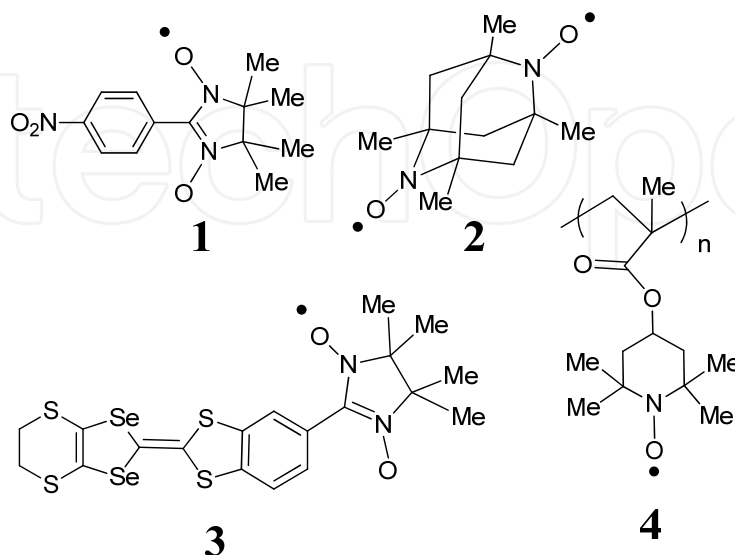


Figure 1. Magnetic materials based on NR chemistry.

Thus, stable NR structures have been used as the spin source or the redox species to develop metal-free solid-state magnetic materials and spintronic devices, or polymer battery devices, respectively. However, the large electric dipole moment (ca. 3 Debye) of a nitroxyl group (N-O•) has never been utilized in these NR-based materials. In this context, with a view to exploiting metal-free magnetic or spintronic soft materials, we have been developing organic liquid-crystalline (LC) and ionic liquid (IL) NRs which can benefit from the unique magnetic and electric properties intrinsic to the NR structure.

Paramagnetic LC compounds have been expected to become novel advanced soft materials that can combine the optical and electrical properties of conventional LCs with the magnetic and electronic properties of paramagnetic compounds (Dunmur & Toriyama, 1999). The magnetic liquid crystals (LCs) are classified into two types; the majority were metal-containing LCs (metallomesogens) with permanent spins originating from transition (d-block) or lanthanide (f-block) metal ions in the mesogen core (Figure 2) (Hudson & Maitlis, 1993; Griesar & Haase, 1999; Binnemans & Gröller-Walrand, 2002; Piguet et al., 2006; Terrazi et al., 2006), while only several all-organic radical LC materials of the first generation were prepared before 2004 (Figure 3), because of the difficulty in the molecular design and synthesis which must satisfy the molecular linearity or planarity necessary for the existence of LC phases (rod-like or disk-like molecules, respectively) as well as the radical stabilization (Kaszynski, 1999; Tamura et al., 2008a, 2012). Moreover, endowing the magnetic LCs with chirality is expected to result in the emergence of unique magneto-electric or magneto-optical properties, intriguing magnetic interactions and so on in the LC state (Tamura et al., 2008b, 2012).

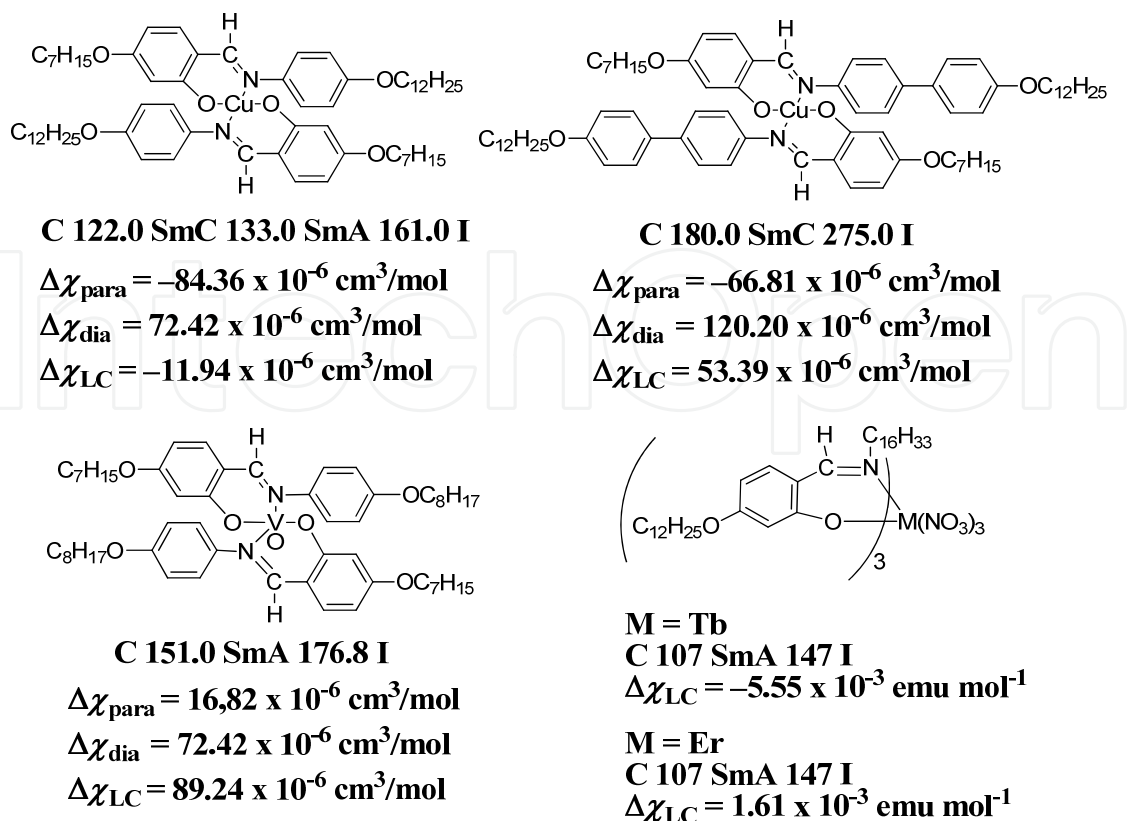


Figure 2. Representative metallomesogens and their transition temperatures and magnetic anisotropies.

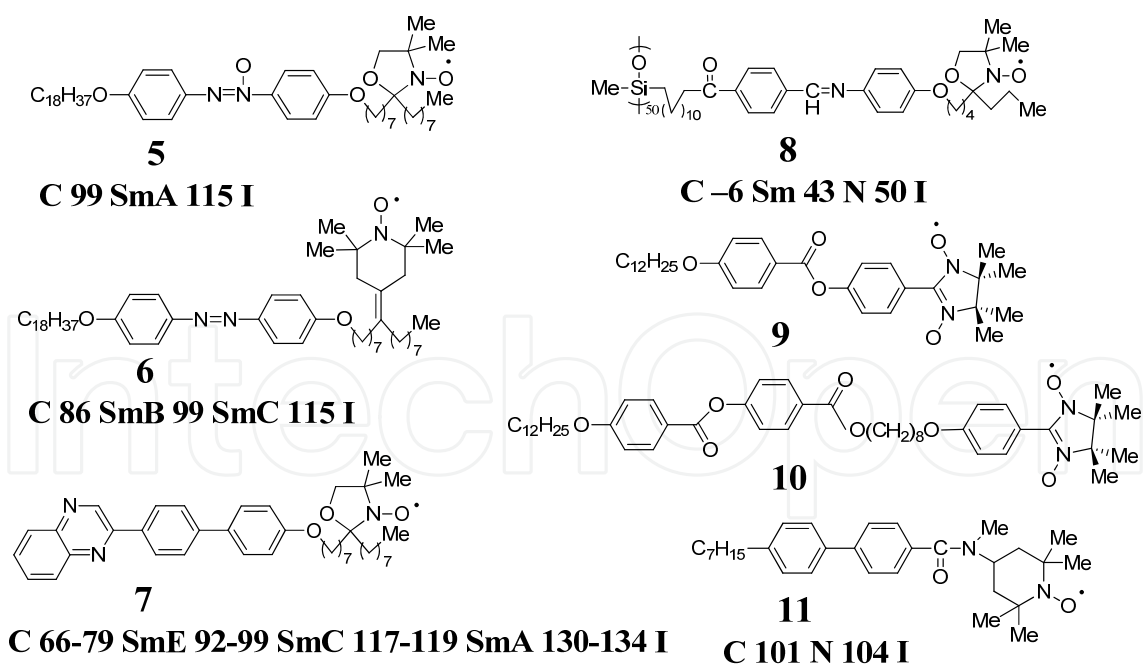


Figure 3. First-generation of rod-like all-organic radical LC compounds 5-11 and their transition temperatures.

In 2004, the present authors reported the preparation and magnetic properties of the prototypic second generation of paramagnetic all-organic rod-like LC compounds **12**, which

contain a chiral cyclic NR (PROXYL) unit in the mesogen core and show various chiral and achiral LC phases over a wide temperature range (Figure 4) (Ikuma et al., 2004). In 2006, the chiral smectic C (SmC*) phase of (2*S*,5*S*)-**12** was found to successfully exhibit ferroelectricity in a thin sandwich cell (Ikuma et al., 2006a, 2006b). Furthermore, quite recently, a sort of spin glass (SG)-like inhomogeneous magnetic interactions (the average spin-spin interaction constant $\bar{J} > 0$), which has been referred to as positive ‘magneto-LC effects’, have been found to be generated in the various chiral and achiral LC phases of compounds **12** and **13** at high temperatures ($> 25\text{ }^\circ\text{C}$) under weak magnetic fields (Uchida et al., 2008, 2010; Suzuki et al., 2012). In fact, these LC droplets floating on water were attracted by a permanent magnet and moved freely on water under the influence of an ordinary permanent magnet (Figure 5).

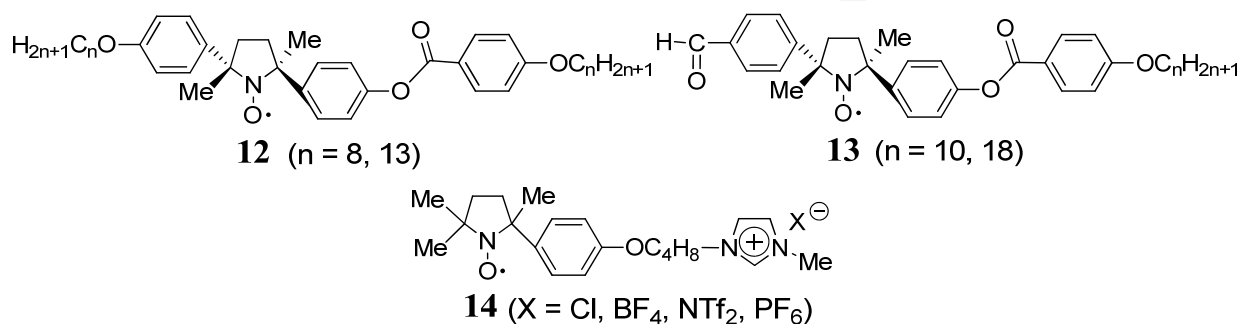


Figure 4. Chiral NR LC compounds **12** and **13**, and IL compounds **14** containing a PROXYL unit.

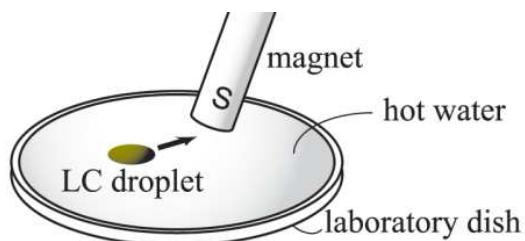


Figure 5. Schematic representation of the attraction by a permanent magnet (maximum 0.5 T) of magnetic LC droplets of **12** and **13** on water in a shallow laboratory dish. Reprinted with permission from ref. (Uchida et al., 2010). Copyright 2012 American chemical Society.

Meanwhile, with the aim of developing room-temperature ionic liquids (ILs) as another type of air-stable, metal-free magnetic soft materials which can act as redox materials or spin probes with molecular shape anisotropy, we designed and synthesized imidazolium compounds **14** containing a chiral PROXYL unit at some distance (Uchida et al., 2009a).

In this chapter, first we briefly introduce the first-generation of all-organic NR LCs, which were prepared before 2004. Then, we report the magnetic and electric properties of the second-generation of NR LCs of compounds **12** and **13**, and the NR IL compounds **14**.

2. First-generation of rod-like all-organic NR LCs

Only a few all-organic radical LC compounds have been prepared, most likely because the geometry and bulkiness of the radical-stabilizing substituents are detrimental to the

stability of LCs, which requires molecular linearity or planarity (Kaszynski, 1999). Although several achiral rod-like organic LCs with a stable cyclic NR (DOXYL or TEMPO) unit as the spin source were prepared (Figure 3), their molecular structures were limited to those containing the NR unit within the terminal alkyl chain, away from the rigid core, and hence allowed the free rotation of the NR moiety inside the molecule, resulting in a decrease in the paramagnetic anisotropy ($\Delta\chi_{\text{para}}$) as well as the dielectric anisotropy ($\Delta\epsilon$) of the whole molecule. The molecular structures and magnetic properties of such first-generation of all-organic NR LCs and the objectives of individual studies are briefly summarized below.

Chiral racemic and achiral compounds **5-7** were synthesized by Dvolaitzky et al. to use them as an LC spin-probe for EPR spectroscopic study. Racemic **7** showed stable achiral smectic phases such as SmA, SmC and SmE (Dvolaitzky et al., 1974, 1976a, 1976b). Their temperature dependence of the molar magnetic susceptibility (χ_{M}) was not measured.

Finkelmann et al. prepared chiral racemic radical polymer **8** which can retain the LC structure in the supercooled glassy phase to measure the magnetic properties of an LC structure at low temperatures (Allgaier & Finkelmann, 1994). The temperature dependence of the χ_{M} was measured by using a Faraday balance in the temperature range from 6 to 350 K, in which the crystal-to-LC-to-liquid phase transition occurred. As a result, **8** showed neither molecular reorientation nor appreciable change in χ_{M} at the crystal-to-LC phase transition temperature in the heating run. This is most likely ascribed to the high viscosity of the polymer material.

Greve et al. synthesized the first LC compounds **9** and **10** with an α -nitronyl nitroxide (α -NN) structure as a spin source at a terminal position in the molecule (Greve et al., 2002). They showed a highly viscous monotropic (irreversible) LC phase in the narrow temperature range from 36 to 39 °C in the heating run. The temperature dependence of the χ_{M} was not measured.

To prepare a supercooled glassy material and crystal polymorphs in the applied magnetic fields and to observe the change in the magnetic behavior accompanying the alteration in the solid-state structure, Nakatsuji et al. synthesized the achiral LC compound **11** (Nakatsuji et al., 2002). Although **11** showed the achiral nematic (N) phase within a narrow temperature range of 3 degree in the heating run, a small but distinct increase in χ_{M} was observed at the crystal-to-LC transition temperature. The difference in the magnetic behavior between the heating and cooling runs was also observed; **11** showed antiferromagnetic interactions according to a singlet-triplet model at low temperatures before the thermal phase transition in the heating run of the crystals, while the magnetic behavior obeyed the Curie-Weiss law in the cooling run from the isotropic phase (Eq. 1).

$$\chi_{\text{para}} = C / (T - \theta) \quad (1)$$

where C is Curie constant, T is temperature, and θ is Weiss temperature.

3. Second-generation of rod-like all-organic NR LCs

3.1. Molecular design and synthesis

The second-generation of chiral NR molecules **12** that could satisfy the following four mandatory requirements were designed and synthesized (Tamura et al., 2008a, 2008b, 2012).

Spin source: A nitroxyl group with a large electric dipole moment (ca. 3 Debye) and known principal g -values (g_{xx} , g_{yy} , g_{zz}) should be the best spin source, because i) the dipole moment is large enough for the source of the spontaneous polarization (P_s) and ii) the principal g -values are useful to determine the direction of molecular alignment in the LC phase by EPR spectroscopy (Figure 6).

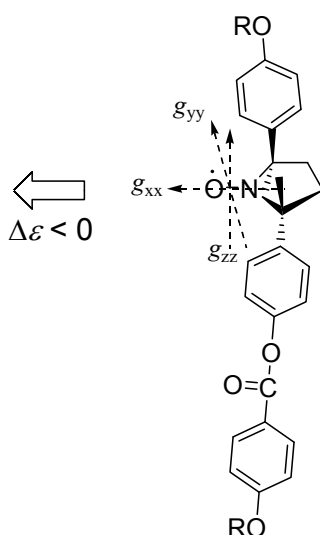


Figure 6. Principal g -values and dielectric anisotropy in the NR molecules **12**.

High thermal stability: A molecule with a 2,2,5,5-tetraalkyl-substituted pyrrolidine-1-oxyl (PROXYL) unit is stable enough for repeated heating and cooling cycles below 150 °C in the air.

Molecular structure: (a) To avoid the free rotation of the NR portion inside the molecule so as to maximize the $\Delta\chi_{\text{para}}$ and $\Delta\epsilon$, a geometrically fixed chiral cyclic NR unit should be incorporated into the rigid core of LC molecules. (b) To obtain a slightly zigzag molecular structure and a negative $\Delta\epsilon$ advantageous for the appearance of a chiral smectic C (SmC^*) phase, a *trans*-2,5-dimethyl-2,5-diphenylpyrrolidine-1-oxyl skeleton in which the electric dipole moment orients to the molecular short axis is the best choice (Figure 6).

Chirality: Since both chiral and achiral LCs are required for comparison of their optical and magnetic properties in various LC phases, the molecules should be chiral and both enantiomerically-enriched and racemic samples need to be available.

3.2. Magnetic properties

Since the magnetic properties such as $\Delta\chi$ -controlled molecular reorientation and magnetic interactions in all-organic magnetic LC phases have been fully characterized for the first

time by using the various LC phases of NR compounds **12**, these experimental results are described in detail.

3.2.1. Magnetic anisotropy of LC compounds

Similarly to $\Delta\epsilon$, $\Delta\chi$ is calculated by subtracting the magnetic susceptibility component (χ_{\perp}) perpendicular to the molecular long axis from the component (χ_{\parallel}) parallel to the same axis (Figure 7 and Eq. 2). Furthermore, the $\Delta\chi$ consists of a paramagnetic component ($\Delta\chi_{\text{para}}$) (Eq. 3) and a diamagnetic component ($\Delta\chi_{\text{dia}}$) (Eq. 4). Although χ_{para} and χ_{dia} are always positive and negative, respectively, $\Delta\chi_{\text{para}}$ and $\Delta\chi_{\text{dia}}$ become positive or negative, depending on the magnitude of the respective χ_{\perp} and χ_{\parallel} values. Accordingly, the overall molecular magnetic anisotropy ($\Delta\chi_{\text{mol}}$) is the sum of $\Delta\chi_{\text{para}}$ and $\Delta\chi_{\text{dia}}$ (Eq. 5) (Griesar & Haase, 1999; Dunmur & Toriyama, 1999). If $\Delta\chi_{\text{mol}}$ is positive (or negative), the molecular long axis becomes parallel (or perpendicular) to the applied magnetic field (H_0), when the applied field is larger than the critical magnetic field (H_c) (Eq. 6 and Figure 7). Such is a driving force for molecular alignment by magnetic fields.

$$\Delta\chi = \chi_{\parallel} - \chi_{\perp} \quad (2)$$

$$\Delta\chi_{\text{para}} = \chi_{\text{para}\parallel} - \chi_{\text{para}\perp} \quad (3)$$

$$\Delta\chi_{\text{dia}} = \chi_{\text{dia}\parallel} - \chi_{\text{dia}\perp} \quad (4)$$

$$\Delta\chi_{\text{mol}} = \Delta\chi_{\text{para}} + \Delta\chi_{\text{dia}} \quad (5)$$

$$H_c = \pi d^{-1} k^{1/2} (\Delta\chi)^{-1/2} \quad (6)$$

where d represents the cell thickness and k is the elastic constant.

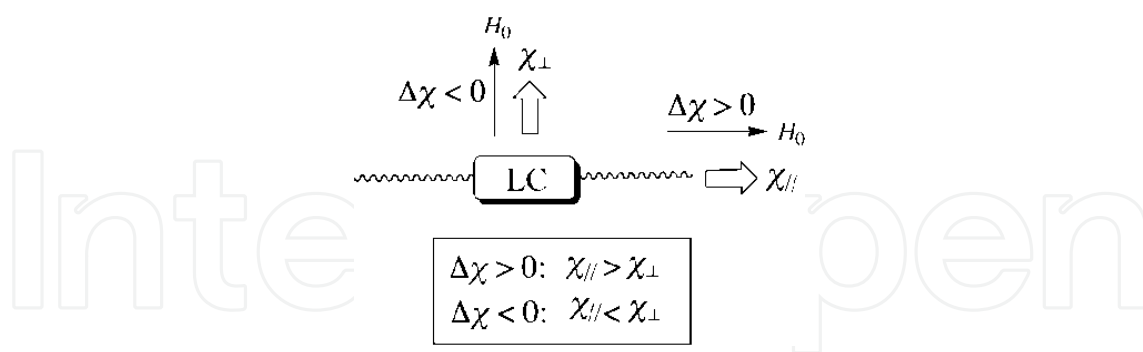


Figure 7. Magnetic anisotropy ($\Delta\chi$) of an LC molecule.

Furthermore, the overall LC magnetic anisotropy ($\Delta\chi_{\text{LC}}$) (Figure 2), which is the sum of $\Delta\chi_{\text{para,LC}}$ and $\Delta\chi_{\text{dia,LC}}$ calculated by EPR spectroscopy and SQUID magnetization measurement, respectively, depends on the orientational order parameter (S) of LCs as shown in Eq. 7 (de Gennes & Prost, 1993).

$$\Delta\chi_{\text{LC}} = N \Delta\chi_{\text{mol}} S \quad (7)$$

where N is the number of molecules.

Diamagnetism resides in all atoms. Particularly aromatic rings show a strong diamagnetic effect in applied magnetic fields. Therefore, the diamagnetic rod-like LC molecules orient themselves such that the axis with the most negative χ_{dia} is perpendicular to the magnetic field. Since $|\chi_{\text{dia}\perp}|$ is usually larger than $|\chi_{\text{dia}\parallel}|$ with regard to organic LC molecules, the $\Delta\chi_{\text{dia}}$ becomes positive and the molecules orient with the director parallel to the magnetic field (Figure 7). For organic LCs, the magnitude of the $\Delta\chi_{\text{dia}}$ which is produced by two diamagnetic phenyl groups is approximately $+50 \times 10^{-6} \text{ emu mol}^{-1}$ (Müller & Haase, 1983). Accordingly, a relatively strong magnetic field ($> 0.2 \text{ T}$) is necessary to align diamagnetic LCs, depending on the type of LC phases (Boamfa et al., 2003). Meanwhile, the $\Delta\chi_{\text{para}}$ of all-organic rod-like LC materials with a stable NR unit in the rigid core is considered to be too small to control the molecular orientation by magnetic fields due to the p-orbital origin.

3.2.2. Magnetic-field-induced molecular alignment

It is known that rod-like metallomesogens with high viscosity are not always suited for the investigation on the alignment of LC molecules by magnetic fields. In contrast, LC compounds **12** with low viscosity, low phase transition temperature, and known principal g -values of the NR moiety are considered to be a good spin-labeled candidate for the studies on the $\Delta\chi$ -controlled molecular orientation by weak magnetic fields. Therefore, to confirm that the magnetic-field-induced molecular alignment in the LC phases of **12** is $\Delta\chi_{\text{dia}}$ -controlled, the $\Delta\chi_{\text{para}}$ and $\Delta\chi_{\text{dia}}$ values of **12** and the approximate magnitude of H_c for each LC phase of **12** were evaluated by EPR spectroscopy and SQUID magnetization measurement and by POM observation under variable magnetic fields, respectively (Uchida et al., 2009b).

First, the temperature-dependent $\Delta\chi_{\text{para}}$ value of compound **12a** ($n=13$) was calculated to be $-1.7 \times 10^{-6} \text{ emu mol}^{-1}$ at 300 K from the g -value obtained by EPR spectroscopy, while the temperature-independent $\Delta\chi_{\text{dia}}$ value was calculated to be $+6.5 \times 10^{-5} \text{ emu mol}^{-1}$ from the experimental molar magnetic susceptibility of $(\pm)\text{-12a}$ measured on a SQUID magnetometer. Thus, $|\chi_{\text{dia}}|$ has turned out to be 30 times larger than $|\chi_{\text{para}}|$; the molecular alignment of **12a** by magnetic fields is definitely $\Delta\chi_{\text{dia}}$ -controlled.

Next, to identify the direction of molecular alignment in the bulk LC state under a weak magnetic field, the temperature dependence of the experimental g -value (g_{exp}) of $(\pm)\text{-12a}$ was measured at a magnetic field of 0.33 T by EPR spectroscopy (Figure 8). In the heating run, the g_{exp} of $(\pm)\text{-12a}$ was constant at around 2.0065 in the crystalline state, then increased at the crystal-to-SmC phase transition, became constant at around 2.0068 in the SmC phase, then decreased abruptly to 2.0058 at the SmC-to-N phase transition, and finally returned to the level (~ 2.0065) of the crystalline state in the isotropic phase. In the cooling run, the g_{exp} of $(\pm)\text{-12a}$ was constant at around 2.0065 in the isotropic phase, then decreased at the Iso-to-N phase transition, became constant at around 2.0055 in the N phase, then increased to 2.0063 at the N-to-SmC phase transition, and finally increased to 2.0067 in the crystalline state.

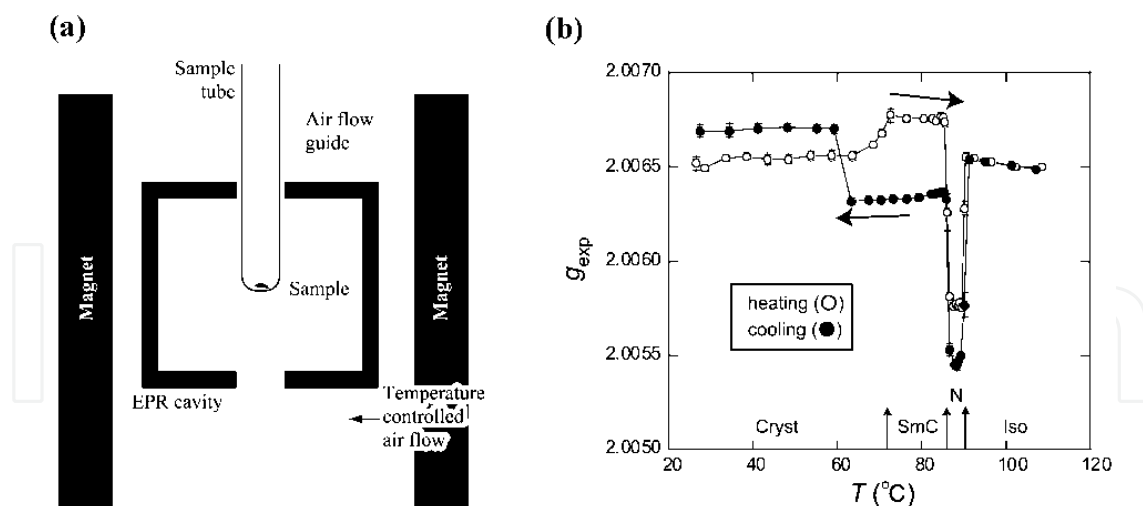


Figure 8. EPR spectroscopy of (\pm) -**12a** ($n=13$). (a) Experimental setup and (b) temperature dependence of the g -value measured through the first heating (white circles) and cooling (black circles) processes. Ref. (Uchida et al., 2009b) – Reproduced by permission of The Royal Society of Chemistry.

From these results and the calculated principal g -values ($g_{\text{iso}}=2.00632$, $g_{\parallel}=2.00540$, $g_{\perp}=2.00678$) of **12a**, it is concluded that i) in the N phase the majority of molecules align their long axis along the applied magnetic field of 0.33 T, owing to the $\Delta\chi_{\text{dia}}$ -controlled molecular reorientation (Figure 9a), whereas in the SmC phase in the heating run the molecular short axis is rather parallel to the field (Figure 9b), most likely due to the viscous layer structure and the natural homeotropic anchoring effect by quartz surface, and ii) that the molecular alignment in each LC phase is influenced by that in the preceding LC phase, although the molecular orientation modes are quite different between the N and SmC phases.

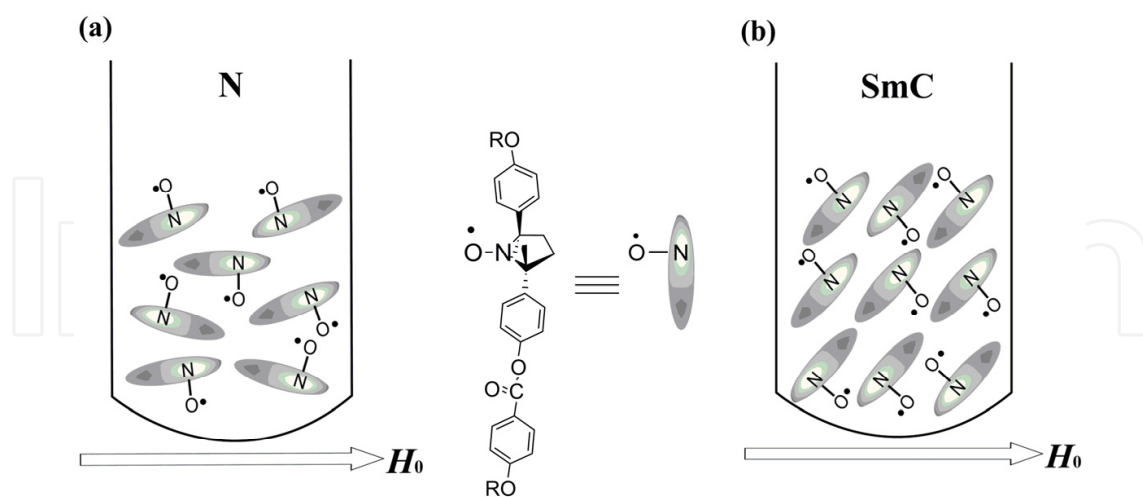


Figure 9. Molecular alignment in the LC phases of (\pm) -**12a** under a weak magnetic field (0.34 T). (a) The N phase in both heating and cooling runs. (b) The SmC phase in the heating run.

To evaluate the H_c for each LC phase of (\pm) -**12a**, we observed the texture change by POM observation under variable magnetic fields. Figure 10 shows the experimental setup: the direction of applied magnetic fields is perpendicular to the LC cell surface. The inner

glass surface in the sandwich cell with 40 μm thickness was neither chemically nor physically treated. The natural Schlieren texture of the N phase gradually became dark with the increasing magnetic field until 0.5 T, resulting in the complete homeotropic orientation of molecules at 1.0 T, whereas the natural Schlieren texture of SmC phase of (\pm)-**12a** scarcely changed below 1.0 T, largely changed between 1.0 T and 1.5 T, and finished the change at less than 2.0 T to show another Schlieren texture (Figure 11), which is similar to the SmC Schlieren texture of (\pm)-**12a** observed under alternative homeotropic boundary conditions (Dierking, 2003). Accordingly, it has been concluded that the smectic layer planes became parallel to the glass plates at 2.0 T. Furthermore, no texture change was noted for N* and SmC* phase of (2*S*,5*S*)-**12a** below 5 T using the same experimental setup.

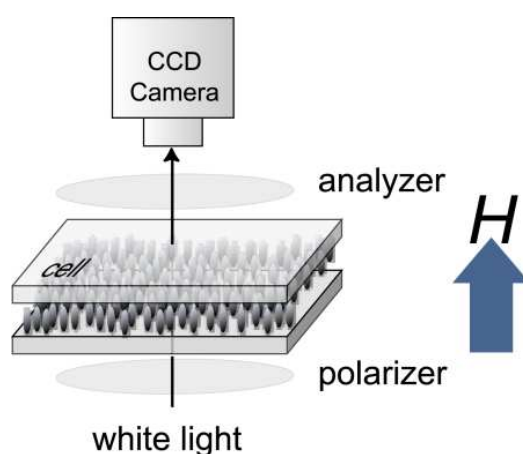


Figure 10. Experimental setup for the polarized optical microscopy observation of (\pm)-**12a** under variable magnetic fields applied perpendicular to the cell surface. Ref. (Uchida et al., 2009b) – Reproduced by permission of The Royal Society of Chemistry.

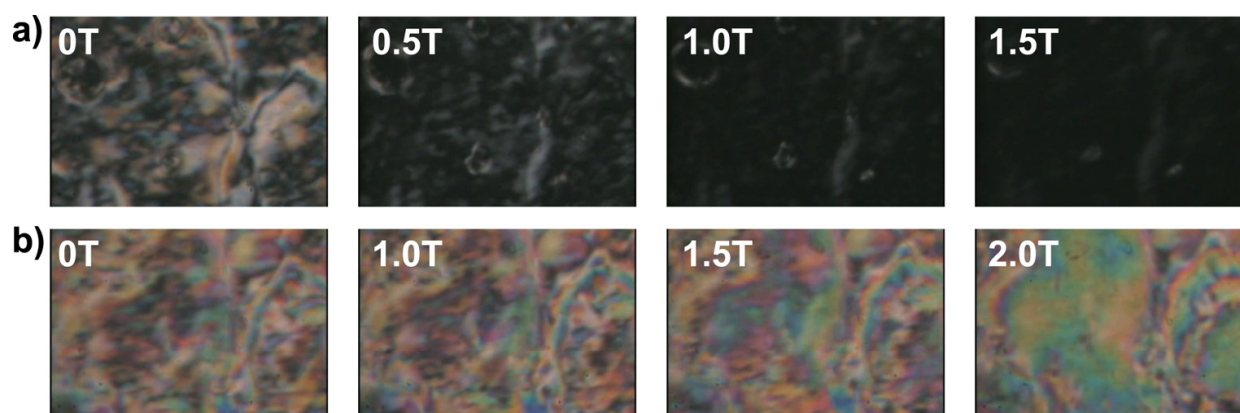


Figure 11. Polarized optical photomicrographs of (\pm)-**12a**. Texture changes (a) from the natural texture to the pseudo-isotropic texture in the N phase at 88.0 $^{\circ}\text{C}$ and (b) from the natural texture to the Schlieren texture in the SmC phase at 83 $^{\circ}\text{C}$, with increasing magnetic fields. Ref. (Uchida et al., 2009b) – Reproduced by permission of The Royal Society of Chemistry.

Thus, the H_c of each LC phase turned out to be largely affected by the superstructure; $H_c(\text{N})$ ($< 1.0 \text{ T}$) $< H_c(\text{SmC})$ ($< 2.0 \text{ T}$) $< H_c(\text{N}^*, \text{SmC}^*)$ ($> 5.0 \text{ T}$).

3.2.3. Magneto-LC effects

The possibility of a ferromagnetic rod-like LC material has been considered unrealistic due to the inaccessibility of long-range spin-spin interactions between rotating molecules in the LC state. However, low viscous all-organic rod-like LC materials with a stable NR unit in the rigid core may show unique intermolecular magnetic interactions owing to the swift coherent collective properties of organic molecules in the LC state.

a. Magnetic LCs with negative dielectric anisotropy ($\Delta\epsilon < 0$)

Interestingly, the present authors observed a nonlinear relationship (S-curve) between the applied magnetic field (H) and the molar magnetization (M) in chiral and achiral LC phases of **12** (Figure 12), which implies the generation of an unusual magnetic interaction in the LC phases under applied magnetic fields (Uchida et al., 2008, 2010). Such a nonlinear relationship was not observed in the crystalline phases of the same compounds which showed a usual linear relationship indicating a paramagnetic nature and no contamination of magnetic impurities in the sample. The in-depth investigation on the magnetic properties of LC compounds **12** strongly suggested that the generation of a sort of spin glass (SG)-like inhomogeneous magnetic interactions (the average spin-spin interaction constant $\bar{J} > 0$), which has been referred to as positive 'magneto-LC effects', induced by weak magnetic

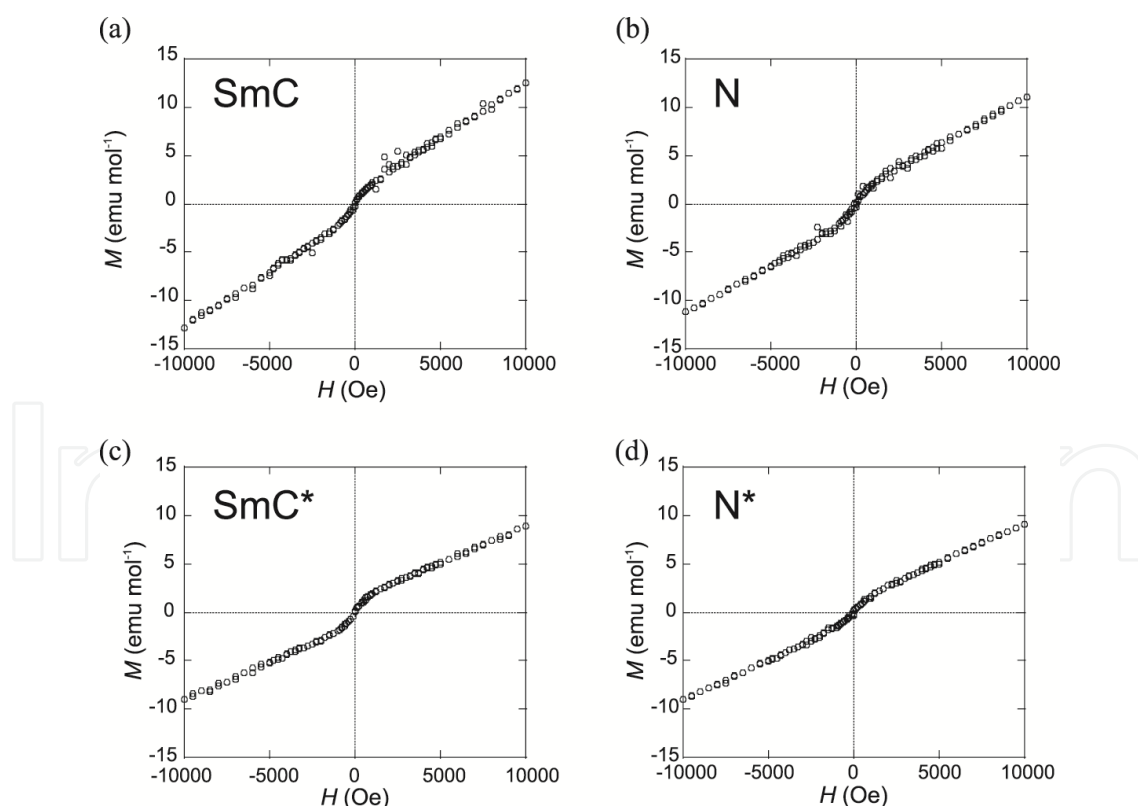


Figure 12. Magnetic field (H) dependence of molar magnetization (M) at 77 °C for (a) the SmC phase of (\pm)-**12a**, (b) the N phase of (\pm)-**12b** ($n=8$), (c) the SmC* phase of (2*S*,5*S*)-**12a** (88% *ee*), and (d) the N* phase of (2*S*,5*S*)-**12b** (96% *ee*). Reprinted with permission from ref. (Uchida et al., 2010). Copyright 2012 American chemical Society.

fields in the various LC phases of compounds **12** is responsible for the observed nonlinear relationship between the H and M ; the magnitude of magnetic interactions depended on the LC phase type, or the superstructure (Figure 13) (Uchida et al., 2010). Furthermore, it was confirmed that the molecular reorientation effect arising from the simple molecular magnetic anisotropy ($\Delta\chi$) has nothing to do with the positive magneto-LC effects observed in the LC phases of **12**. Thus, it was concluded that the origin of such strong SG-like inhomogeneous magnetic interactions can be interpreted in terms of the anisotropic spin-spin dipole interactions induced by weak magnetic fields in the anisotropic LC superstructure.

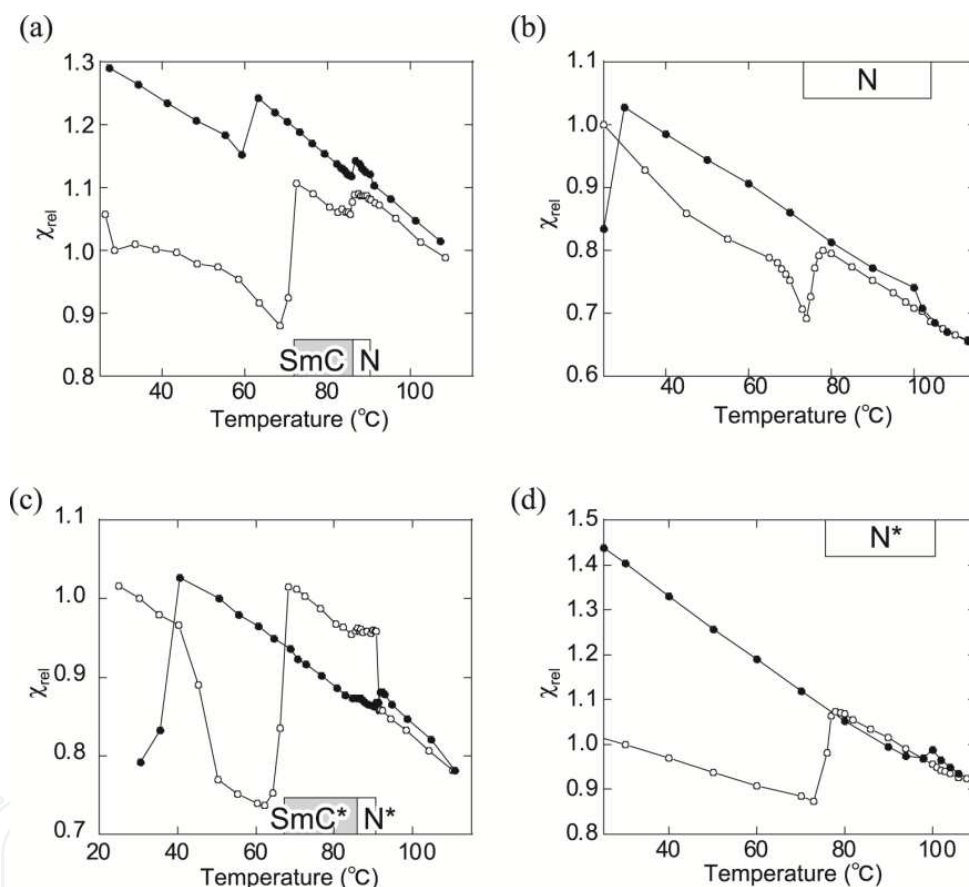


Figure 13. Temperature dependence of relative paramagnetic susceptibility (χ_{rel}) for (a) (\pm)-**12a**, (b) (\pm)-**12b**, (c) (2*S*,5*S*)-**12a** (88% *ee*), and (d) (2*S*,5*S*)-**12b** (96% *ee*) at a magnetic field of 0.33 T. Open and filled circles represent the first heating and cooling runs, respectively. The LC temperatures shown in a box refer to the first heating process. Reprinted with permission from ref. (Uchida et al., 2010). Copyright 2012 American chemical Society.

In this study, we could indicate that EPR spectroscopy is the much better means than SQUID magnetization measurement to evaluate the temperature dependence of the χ_{para} for organic NR LC compounds at high temperatures. This is due to the following four reasons: (i) The χ_{para} can be derived from the Bloch equation (Eq. 8) by using the parameters obtained

from the EPR differential curves, such as maximum peak height (I'_m and $-I'_m$), g -value (g), and peak-to-peak line width (ΔH_{pp}).

$$\chi_{para} = \frac{2\mu_B g I'_m \Delta H_{pp}^2}{\sqrt{3} h \nu H_1} \quad (8)$$

where μ_B is the Bohr magneton, h is Planck's constant, ν is the frequency of the absorbed electromagnetic wave, and H_1 is the amplitude of the oscillating magnetic field. Accordingly, the temperature dependence of relative paramagnetic susceptibility (χ_{rel}), which is defined as

$$\chi_{rel} = \frac{\chi_{para}}{\chi_0} \quad (9)$$

where χ_0 is the standard paramagnetic susceptibility, e.g., at 30°C in the heating run (Eq. 9), can be actually used (Figure 12). (ii) Treatment of the χ_{dia} term is totally unnecessary. (iii) The experimental error is very small even at such high temperatures. (iv) The analysis of microscopic magnetic interactions such as spin-spin dipole and exchange interactions is also feasible.

b. Magnetic LCs with positive dielectric anisotropy ($\Delta\epsilon > 0$)

To examine the effects of $\Delta\epsilon$ on the magneto-LC effects, compounds **13** with a terminal formyl group (Figure 4) which have a positive $\Delta\epsilon$ were synthesized. Under weak magnetic fields, positive magneto-LC effects ($\bar{J} > 0$) operated in the chiral nematic (N*) phase of (2S,5S)-**13a** ($n=10$) and in the smectic A (SmA*) phase of (2S,5S)-**13b** ($n=18$) (Figure 14a,b), whereas negative magneto-LC effects ($\bar{J} < 0$) were observed in the achiral nematic (N) phase of (\pm)-**13a** (Figure 14c) (Suzuki, et al., 2012). The origin of such negative magneto-LC effects operating in the N phase of (\pm)-**13a** was interpreted in terms of the generation of antiferromagnetic interactions which is associated with the formation of the RS magnetic dipolar interaction due to the strong electric dipole interactions (Figure 15c), while ferromagnetic head-to-tail spin-spin dipole interactions should dominate in the N* and SmA* phases (Figure 15a,b).

c. Attraction of magnetic LC droplet by a permanent magnet

Furthermore, these radical LC droplets floating on water were attracted by a permanent magnet and moved freely on water under the influence of this magnet (Figure 5), whereas the crystallized particles of the same compounds never responded to the same magnet. The response of the LC droplets to the magnet also varied depending on the LC phase type, i.e., the extent of the magnetic interaction (\bar{J}). These results indicate that the LC phase domain can help to induce magnetic interactions under applied magnetic fields (Uchida et al., 2008, 2010; Suzuki et al., 2012). This unique magnetic attraction will find use in the development of the metal-free magnetic soft materials usable at ambient temperature, such as a magnetic LC carrier for the magnetically targeted drug-delivery system or an MRI contrast agent (Kumar, 2009).

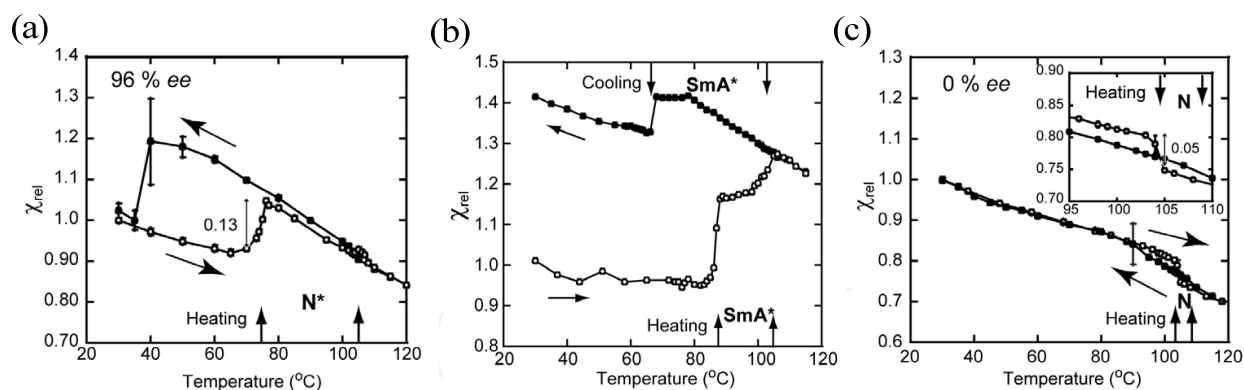


Figure 14. Temperature dependence of χ_{rel} value for (a) (2*S*,5*S*)-**13a**, (b) (2*S*,5*S*)-**13b** and (c) (±)-**13a**. Ref. (Suzuki et al., 2012) – Reproduced by permission of The Royal Society of Chemistry.

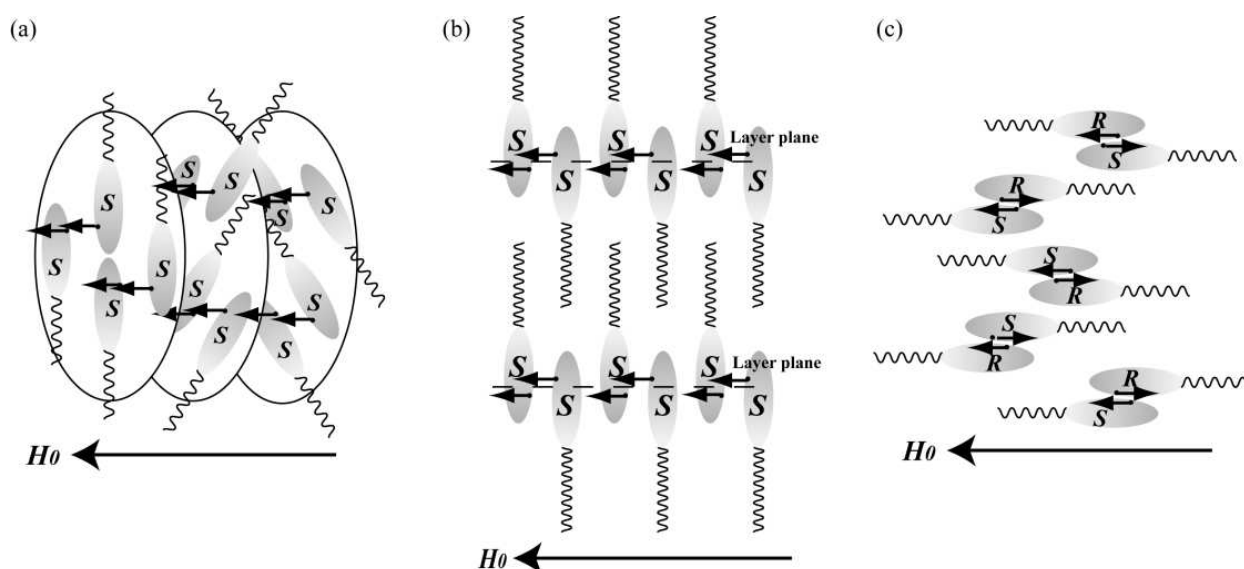


Figure 15. Spin-spin dipole interactions in LC phases. (a) *N** phase of (2*S*,5*S*)-**13a**, (b) *SmA** phase of (2*S*,5*S*)-**13b** and (c) *N* phase of (±)-**13a**. Ref. (Suzuki et al., 2012) – Reproduced by permission of The Royal Society of Chemistry.

3.3. Ferroelectric properties

It is known that when an *SmC** phase is confined to a thin sandwich cell with a gap smaller than the pitch of the helical superstructure, an unwinding of the helix occurs and a bistable, ferroelectric device is formed (Figure 16) (Goodby et al., 1991; Lagerwall, 1999; Dierking, 2003). Consequently, *P_s* is generated in the sandwich cell in which ferroelectric switching occurs by changing the polarity of the electric field. The ferroelectric properties of the *SmC** phase of each sample are characterized by measuring the *P_s*, the optical response time of bistable switching to an applied electric field, and the tilt angle.

The *SmC** phase of (2*S*,5*S*)-**12a** indeed exhibited ferroelectricity in a planar anchoring thin sandwich cell (4 μm thickness) (Ikuma et al, 2006a, 2006b); a *P_s* value of 24 nC cm⁻², an optical response time (τ_{10-90}) of 0.213 msec and a layer tilt angle (θ) of 29° were recorded. The ferroelectric LC data of (2*S*,5*S*)-**12a** were superior to those of the typical chiral

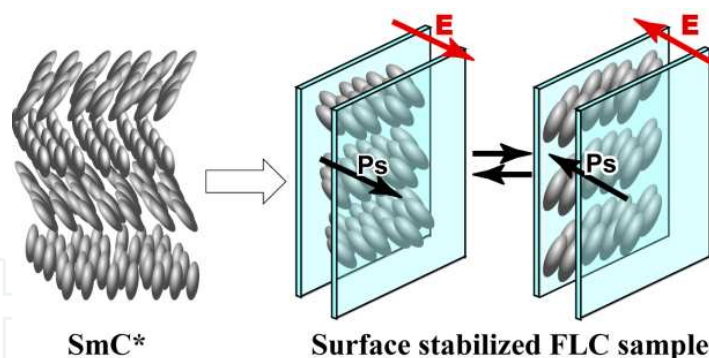
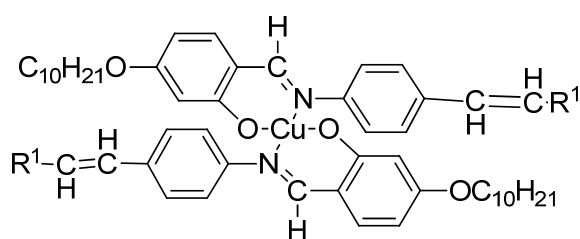


Figure 16. Ferroelectric switching in a thin sandwich cell.

metallomesogen **15** (Figure 17); **15** showed a higher P_s value of 38 nC cm^{-2} with a θ of 23° than (2*S*,5*S*)-**12a**, but the optical response was very slow ($\tau_{10-90} = 8.5 \text{ msec}$) due to the high viscosity (Iglesias et al., 1996).



C 109.2 SmC* 120 SmA 160.1 I

$P_s(-10^\circ\text{C}) = 38 \text{ nC cm}^{-2}$

$\tau(-10^\circ\text{C}) = 8.5 \text{ ms } (4 \text{ V } \mu\text{m}^{-1})$

Figure 17. Ferroelectric metallomesogen **15**.

Furthermore, second-harmonic generation (SHG) was clearly observed by Kogo and Takezoe et al. under a phase-matching condition in the SmC* phase of (2*S*,5*S*)-**12a** loaded into an LC cell ($20 \mu\text{m}$ thickness), validating the existence of ferroelectricity. The effective second-order nonlinear optical (NLO) constant was evaluated to be a $4.8 \times 10^{-2} \text{ pm V}^{-1}$, 3 orders of magnitude smaller than that of quartz known as a standard NLO material (Kogo et al., 2010).

4. NR Ionic Liquids (ILs)

The synthesis and electric, electrochemical and magnetic properties of IL compounds (\pm)-**14** were reported (Figure 4), coupled with the first use of this type of magnetic IL as an EPR spin probe in typical achiral diamagnetic ILs (Uchida et al, 2009a). Although the chloride (\pm)-**14a** ($X = \text{Cl}$) was hygroscopic and miscible with water, anhydrous and fairly hydrophobic ILs were obtained for other salts of (\pm)-**14** ($X = \text{BF}_4, \text{NTf}_2, \text{PF}_6$) which showed a glass transition between -37 and -22°C and decomposed between 162 and 170°C in air.

The temperature dependence of χ_M of the least viscous (\pm)-**14b** ($X = \text{NTf}_2$) measured on a SQUID magnetometer at a field of 0.5 T showed the high radical purity and antiferromagnetic interactions below 10K. Ionic conductivity and viscosity of (\pm)-**14b** were determined to be $5.23 \times 10^{-5} \text{ S cm}^{-1}$ and $1.087 \times 10^{-3} \text{ cP}$, respectively, at 25 °C. Electrochemical studies using cyclic voltammetry (CV) were carried out for a CH_3CN solution (1 mM) of (\pm)-**14b** and the neat IL ($\rho = 1.49 \text{ g cm}^{-3}$; the radical concentration is 2.34 M at 25°C), without an additional supporting electrolyte (Figure 18). The voltammogram measured in CH_3CN exhibited a quasireversible wave with half-wave oxidation potential ($E_{1/2^{\text{ox}}}$) of +0.363 V (*vs.* Fc/Fc^+), while that in the neat IL measured with a micro CV cell showed a wider quasireversible wave with $E_{1/2^{\text{ox}}} = +0.458 \text{ V}$. The diffusion coefficient of **14b** or the corresponding oxoammonium ion in the neat IL was determined to be $2 \times 10^{-10} \text{ cm}^2 \text{ s}^{-1}$. Thus, paramagnetic (\pm)-**14b** with high radical purity turned out to be air-stable room temperature IL which can exhibit ionic conductivity and a quasireversible redox behavior in the absence of additional solvent and electrolyte. Notably, (\pm)-**14b** with molecular shape anisotropy proved to serve as the first IL EPR spin probe that can recognize the local structure or the molecular shape anisotropy of achiral diamagnetic IL solvents.

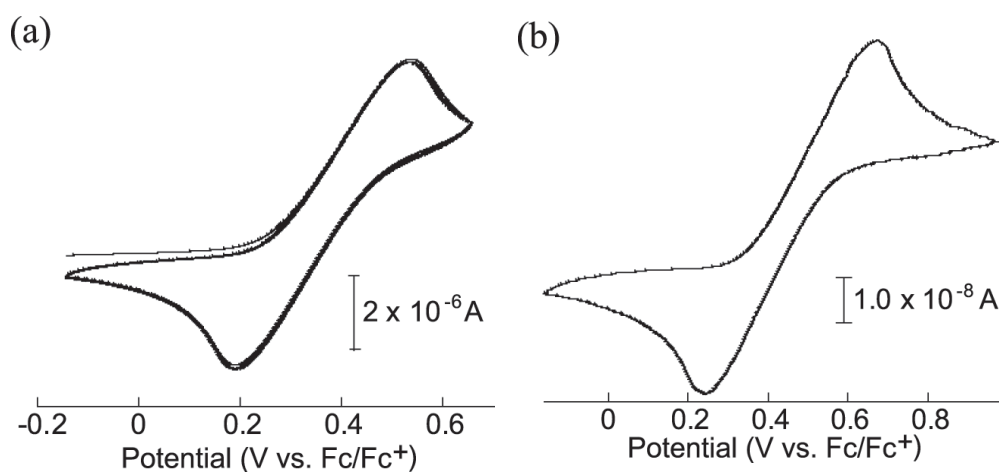


Figure 18. Cyclic voltammograms of (\pm)-**14b** recorded at 25°C for (a) the MeCN solution (1.0 mM) at a scan rate of 100 mV s^{-1} (five scans) using Pt working and counter electrodes and an Ag reference electrode without an additional supporting electrolyte and (b) the neat ionic liquid sample at a scan rate of 0.5 mV s^{-1} (single scan) using a micro cell with Pt working, counter and reference electrodes without solvent and an additional supporting electrolyte. Ref. (Uchida et al., 2009a) – Reproduced by permission of The Royal Society of Chemistry.

5. Conclusions and prospects

The unique magnetic and electric properties of organic NR LCs and ILs were briefly surveyed. Noteworthy is the first observation of positive magneto-LC effects ($\bar{J} > 0$) under weak magnetic fields in both chiral and achiral rod-like LC phases of the second-generation of all-organic NR compounds **12** with negative dielectric anisotropy ($\Delta\epsilon < 0$), while positive and negative magneto-LC effects ($\bar{J} > 0$ and $\bar{J} < 0$) were observed in the chiral and achiral

LC phases of **13**, respectively, with positive dielectric anisotropy ($\Delta\epsilon > 0$). Meanwhile, the ferroelectric properties of the SmC* phase of **12a** were fully characterized in a thin sandwich cell; the NR unit proved to act as the sufficient source of spontaneous polarization (P_s). Such chiral organic NR LCs with low viscosity showed faster ferroelectric switching than chiral metallomesogens with high viscosity. The control of magnetic properties of magnetic ferroelectric LCs of **12** by electric fields is the next step. In addition, it is of great advantage to be able to use EPR spectroscopy as the tool for observing the microscopic dynamic behavior of molecules in the NR LC phases, coupled with the use of SQUID magnetization measurement to observe the macroscopic behavior. Furthermore, EPR spectroscopy turned out to be an excellent tool for analyzing the temperature dependence of the χ_{para} for organic NR LC phases at high temperatures, for which SQUID magnetization measurement is not suited. Thus, such second generation of all-organic chiral LC NR compounds would open up a novel research field of metal-free magnetic or spintronic LC materials.

Meanwhile, the advent of IL NR EPR spin probes would make possible the in-depth understanding of the local structure or the molecular shape anisotropy of diamagnetic IL solvents, which cannot be available by using conventional spin probes such as TEMPO derivatives.

The research on metal-free magnetic soft materials is still in its infancy. The development of novel metal-free magnetic soft materials such as LCs, ILs, emulsions, and gels based on the NR chemistry is strongly expected.

Author details

Rui Tamura, Yoshiaki Uchida and Katsuaki Suzuki

Graduate School of Human and Environmental Studies, Kyoto University, Japan

Acknowledgement

We Acknowledge Professor Takeji Takui, Professor Hiroyuki Nohira, Dr. Yoshio Aoki, Professor Hideo Takezoe, Dr. Yoshio Shimbo, Ms. Reiri Kogo, Professor Jun Yamauchi, Dr. Yohei Noda, Dr. Naohiko Ikuma and Dr. Satoshi Shimono for their collaboration.

6. References

- Allgaier, J. & Finkelmann, H. (1994). Synthesis and Magnetic Properties of Mesogenic Side-Chain Polymers Containing Stable Radicals, *Macromolecular Chemistry and Physics*, Vol.195, pp. 1017-1030.
- Amabilino, D. B & Veciana, J. (2001). Nitroxide-Based Organic Magnets, In: *Magnetism: Molecules to Materials II*, J.S.Miller & M.Drillon, (Eds.), 1-60, Wiley-VCH, ISBN 3-527-30301-4, Weinheim, Germany.
- Aurich, H. G. (1989). Nitroxides, In: *Nitrones, Nitronates and Nitroxides*, E.Breuer, H.G.Aurich, A.Nielsen, (Eds.), 313-370, John Wiley & Sons, ISBN 0-471-91709-5, Chichester, UK.

- Binnemans, K. & Gröller-Walrand, C. (2002). *Lanthanide-Containing Liquid Crystals and Surfactants*, Chemical Reviews, Vol.102, pp.2303-2345.
- Boamfa, M. I.; Kim, M. W.; Maan, J. C. & Rasing, T. (2003). Observation of Surface and Bulk Phase Transitions in Nematic Liquid Crystals, *Nature*, Vol.421, 149-152.
- Chiarelli, R.; Novak, M. A.; Rassat, A. & Tholence, J. L. (1993). A Ferromagnetic Transition at 1.48 K in an Organic Nitroxide. *Nature*, Vol. 363, pp. 147-149.
- De Gennes, P. G. & Prost, J. (1993). *The Physics of Liquid Crystals*, Oxford University Press, ISBN 0-19-852024-7, New York, USA.
- Dierking, I. (2003). *Textures of Liquid Crystals*, Wiley-VCH, ISBN 3-527-30725-7, Weinheim, Germany.
- Dunmur, D. & Toriyama, K. (1999). Magnetic Properties of Liquid Crystals, In: *Physical Properties of Liquid Crystals*, D.Demus, J.Goodby, G.W.Gray, H.-W.Spiess, V.Vill, (Eds.), 102-112, Wiley-VCH, ISBN 3-527-29747-2, Weinheim, Germany.
- Dvolaitzky, M.; Billard, J. & Poldy, F. (1974). Notes des Membres et Correspondants et Notes Présentées ou transmises par Leurs Soins, *Comptes Rendus de L'académie des Science*, Vol. 279C, pp.533-535.
- Dvolaitzky, M.; Billard, J. & Poldy, F. (1976b). Smectic E, C and A Free Radicals, *Tetrahedron*, Vol. 32, 1835-1838.
- Dvolaitzky, M.; Taupin, C. & Poldy, F. (1976a). Nitroxides Piperidiniques – Synthèse de Nouvelles Sondes Paramagnetiques, *Tetrahedron Letters*, pp. 1469-1472.
- Goodby, J. W.; Blinc, R.; Clark, N. A.; Lagerwall, S. T.; Osipov, M. A.; Pikin, S. A.; Sakurai T.; Yoshino, K. & Boštjan, Ž. (1991). *Ferroelectric Liquid Crystals*, Gordon and Breach Science Publishers, ISBN 2-88124-282-0, Philadelphia, USA.
- Greve, S.; Vill, V. & Friedrichsen, W. (2002). Novel Nitronyl Nitroxides: Synthesis and Properties, *Zeitschrift für Naturforschung*, Vol.57b, pp. 677-684.
- Griesar, K. & Haase, W. (1999). Magnetic Properties of Transition-Metal-Containing Liquid Crystals, In: *Magnetic Properties of Organic Materials*, P.M.Lahti, (Ed.), 325-344, Marcel Dekker, ISBN 0-8247-1976-X, New York, USA.
- Hicks, R. G. (2010) (Ed). *Sable Radicals: Fundamentals and Applied Aspects of Odd-Electron Compounds*, John Wiley & Sons, ISBN 978-0-470-77083-2, Chichester, UK.
- Hudson, S. A. & Maitlis, P. M. (1993). Calamitic Metallomesogens: Metal-Containing Liquid Crystals with Rodlike Shapes. *Chemical Reviews*, Vol.93, pp. 861-885.
- Iglesias, R.; Marcos, M.; Martinez, J.; Serrano, J. L.; Sierra, T. & Perez-Jubindo, M. A. (1996). Ferroelectric Behavior of Chiral Bis(salicylideneaniline) Copper(II), Vanadium(IV), and Palladium(II) Liquid Crystals, *Chemistry of Materials*, Vol.8, pp. 2611-2617.
- Ikuma, N.; Tamura, R.; Masaki, K.; Uchida, Y.; Shimono, S.; Yamauchi, J.; Aoki, Y. & Nohira, H. (2006b). Paramagnetic FLCs Containing an Organic Radical Component, *Ferroelectrics*, Vol.343, 119-125.
- Ikuma, N.; Tamura, R.; Shimono, S.; Kawame, N.; Tamada, O.; Sakai, N.; Yamauchi, J. & Yamamoto, Y. (2004). Magnetic Properties of All-Organic Liquid Crystals Containing a Chiral Five-Membered Cyclic Nitroxide Unit within the Rigid Core, *Angewandte Chemie International Edition*, Vol.43, 3677-3682.

- Ikuma, N.; Tamura, R.; Shiono, S.; Uchida, Y.; Masaki, K.; Yamauchi, J.; Aoki, Y. & Nohira, H. (2006a). Ferroelectric Properties of Paramagnetic, All-Organic, Chiral Nitroxyl Radical Liquid Crystals, *Advanced Materials*, Vol.18, 477-480.
- Kaszynski, P. (1999). Liquid Crystalline Radicals: An Emerging Class of Organic Magnetic Materials, In: *Magnetic Properties of Organic Materials*, P.M.Lahti, (Ed.), 325-344, Marcel Dekker, ISBN 0-8247-1976-X, New York, USA.
- Kogo, R.; Araoka, F.; Uchida, Y.; Tamura, R.; Ishikawa, K. & Takezoe, H. (2010). Second Harmonic Generation in a Paramagnetic All-Organic Chiral Smectic Liquid Crystal, *Applied Physics Express*, Vol.3, 041701.
- Kumar, C. K. (Ed). (2009). *Magnetic Nanomaterials*, Wiley-VCH, ISBN 978-3-527-32154-4, Weinheim, Germany.
- Lagerwall, S. T. (1999), *Ferroelectric and Antiferroelectric Liquid Crystals*, Wiley-VCH, ISBN 3-527-29831-2, Weinheim, Germany.
- Matsushita, M. M.; Kawakami, H.; Kawada, Y. & Sugawara, T. (2007). Negative Magneto-Resistance Observed on an Ion-Radical Salt of a TTF-Based Spin-Polarized Donor. *Chemistry Letters*, pp. 110-111.
- Matsushita, M. M.; Kawakami, H.; Sugawara, T. & Ogata, M. (2008). Molecule-Based System with Coexisting Conductivity and Magnetism and Without Magnetic Inorganic Ions. *Physical Review. B*, Vol.77, 195208.
- Müller, H. J. & Haase, W. (1983). Magnetic Susceptibility and the Order Parameter of Some 4,4'-Disubstituted Biphenyl Cyclohexanes, *Journal de Physique (Paris)*, Vol.44, pp. 1209-1213.
- Nakahara, K.; Iwasa, S.; Satoh, M.; Morioka, Y.; Iriyama, J.; Suguro, M. & Hasegawa, E. (2002). Rechargeable Batteries with Organic Radical Cathodes. *Chemical Physics Letters*, Vol.359, pp. 351-354.
- Nakatsuji, S. (2008). Preparation, Reactions, and Properties of Functional Nitroxide Radicals, In: *Nitroxides: Applications in Chemistry, Biomedicine, and Materials Science*, G.I.Likhtenshtein, J.Yamauchi, S.Nakatsuji, A.I.Smirnov & R.Tamura, (Eds.), 161-204, Wiley-VCH, ISBN 978-3-31889-6, Weinheim, Germany.
- Nakatsuji, S.; Mizumoto, M.; Ikemoto, H.; Akutsu, H. & Yamada, J. (2002). Preparation and Properties of Organic Radical Compounds with Mesogenic Cores, *European Journal of Organic Chemistry*, pp. 1912-1918.
- Oyaizu, K. & Nishide, H. (2010). Mesoscale Radical Polymers: Bottom-Up Fabrication of Electrodes in Organic Polymer Batteries, In: *Advanced Nanomaterials*, Vol.2, K.E.Geckeler, H.Nishide, (Eds.), 319-332, Wiley-VCH, ISBN 978-3-527-31794-3, Weinheim, Germany.
- Piguet, C.; Bünzli, J-C. G.; Donnio, B. & Guillon, D. (2006). Thermotropic Lanthanidomesogens, *Chemical Communications*, pp. 3755-3768.
- Suga, T. & Nishide, H. (2010). Rechargeable Batteries Using Robust but Redox Active Organic Radicals, In: *Sable Radicals: Fundamentals and Applied Aspects of Odd-Electron Compounds*, R.G.Hicks, (Ed.), 507-520, John Wiley & Sons, ISBN 978-0-470-77083-2, Chichester, UK.

- Sugawara, T.; Komatsu, H. & Suzuki, K. (2011). Interplay between Magnetism and Conductivity Derived from Spin-Polarized Donor Radicals. *Chemical Society Reviews*, Vol.40, pp. 3105-3118.
- Suzuki, K.; Uchida, Y.; Tamura, R.; Shimono, S. & Yamauchi, J. (2012). Observation of Positive and Negative Magneto-LC Effects in All-Organic Nitroxide Radical Liquid Crystals by EPR Spectroscopy, *Journal of Materials Chemistry*, DOI: 10.1039/c2jm16278d.
- Tamura, M.; Nakazawa, Y.; Shiomi, D.; Nozawa, K.; Hosokoshi, Y.; Ishikawa, M.; Takahashi, M. & Kinoshita, M. (1991). Bulk Ferromagnetism in the β -Phase Crystal of the *p*-Nitrophenyl Nitronyl Nitroxide Radical. *Chemical Physics Letters*, Vol.186, No.4 & 5, pp. 401-404.
- Tamura, R. (2008a). Organic Functional Materials Containing Nitroxide Radical Units, In: *Nitroxides: Applications in Chemistry, Biomedicine, and Materials Science*, G.I.Likhtenshtein, J.Yamauchi, S.Nakatsuji, A.I.Smirnov & R.Tamura, (Eds.), 303-329, Wiley-VCH, ISBN 978-3-31889-6, Weinheim, Germany.
- Tamura, R.; Uchida, Y. & Ikuma, N. (2008b). Paramagnetic All-Organic Chiral Liquid Crystals, *Journal of Materials Chemistry*, Vol.18, pp. 2872-2876.
- Tamura, R.; Uchida, Y. & Suzuki, K. (2012). Magnetic Liquid Crystals, In: *Liquid Crystals Beyond Displays: Chemistry, Physics, and Applications*, Q, Li (Ed.), Chap. 3, John Wiley & Sons, ISBN 978-1-118-07861-7, Chichester, UK.
- Terazzi, E.; Suarez, S.; Torelli, S.; Nozary, H.; Imbert, D.; Mamula, O.; Rivera, J-P.; Guillet, E.; Bénech, J-M.; Bernardinelli, G.; Scopelliti, R.; Donnio, B.; Guillon, D.; Bünzli, J-C. G. & Piguet, C. (2006). Introducing Bulky Functional Lanthanide Cores into Thermotropic Metallomesogens: A Bottom-Up Approach. *Advanced Functional Materials*, Vol.16, pp. 157-168.
- Uchida, Y.; Ikuma, N.; Tamura, R.; Shimono, S.; Noda, Y.; Yamauchi, J.; Aoki, Y. & Nohira, H. (2008). Unusual Intermolecular Magnetic Interaction Observed in an All-Organic Radical Liquid Crystal, *Journal of Materials Chemistry*, Vol.18, pp. 2950-2952.
- Uchida, Y.; Oki, S.; Tamura, R.; Sakaguchi, T.; Suzuki, K.; Ishibashi, K. & Yamauchi, J. (2009a). Electric, Electrochemical and Magnetic Properties of Novel Ionic Liquid Nitroxides, and Their Use as an EPR Spin Probe. *Journal of Materials Chemistry*, Vol.19, pp. 6877-6881.
- Uchida, Y.; Suzuki, K.; Tamura, R.; Ikuma, N.; Shimono, S.; Noda, Y. & Yamauchi, J. (2010). Anisotropic and Inhomogeneous Magnetic Interactions Observed in All-Organic Nitroxide Radical Liquid Crystals, *Journal of the American Chemical Society*, Vol.132, 9746-9752.
- Uchida, Y.; Tamura, R.; Ikuma, N.; Shimono, S.; Yamauchi, J.; Shimbo, Y.; Takezoe, H.; Aoki, Y. & Nohira, H. (2009b). Magnetic-Field-Induced Molecular Alignment in an Achiral Liquid Crystal Spin-Labeled by a Nitroxyl Group in the Mesogen Core, *Journal of Materials Chemistry*, Vol.19, pp.415-418.